Journal of Power Sources 196 (2011) 9213–9219

Contents lists available at ScienceDirect

Journal of Power Sources

journal homepage: www.elsevier.com/locate/jpowsour

Analysis of carbon fiber brush loading in anodes on startup and performance of microbial fuel cells

Adam J. Hutchinson, Justin C. Tokash, Bruce E. Logan*

Department of Civil and Environmental Engineering, Penn State University, University Park, PA 16802, USA

ARTICLE INFO

Article history:
Received 7 June 2011
Received in revised form 9 July 2011
Accepted 11 July 2011
Available online 20 July 2011

Keywords:
Microbial fuel cell
Carbon fiber brush anodes
Internal resistance
Electrochemical impedance spectroscopy

ABSTRACT

Flat carbon anodes placed near a cathode in a microbial fuel cell (MFC) are adversely affected by oxygen crossover, but graphite fiber brush anodes placed near the cathode produce high power densities. The impact of the brush size and electrode spacing was examined by varying the distance of the brush end from the cathode and solution conductivity in multiple MFCs. The startup time was increased from 8 ± 1 days with full brushes (all buffer concentrations) to 13 days (50 mM), 14 days (25 mM) and 21 days (8 mM) when 75% of the brush anode was removed. When MFCs were all first acclimated with a full brush, up to 65% of the brush material could be removed without appreciably altering maximum power. Electrochemical impedance spectroscopy (EIS) showed that the main source of internal resistance (IR) was diffusion resistance, which together with solution resistance reached 100 Ω. The IR using EIS compared well with that obtained using the polarization data slope method, indicating no major components of IR were missed. These results show that using full brush anodes avoids adverse effects of oxygen crossover during startup, although brushes are much larger than needed to sustain high power.

1. Introduction

MFCs have received considerable attention recently because they can be used to produce electricity while simultaneously cleaning waste water, making them a single solution to two significant environmental challenges [1]. Increased power densities are needed in MFCs, and many improvements have been obtained through modifying system architecture, materials, and through a better understanding of solution chemistry on performance [2]. One of these advances has been the use of a graphite fiber brush anode. This type of electrode provides a high surface area for bacterial adhesion and biofilm formation, and highly porous brush improves power generation compared to more traditional flat carbon anode materials [3,4]. When the anode and cathode are placed closer together the solution resistance is reduced and power should remain constant or increase. However, when a flat anode is placed near an air cathode (typically at a distance of less than 2 cm) in an MFC lacking a membrane or separator, the power density decreases due to oxygen contamination of the anode [5,6]. Brush anodes do not exhibit this behavior of decreased power with electrode spacing, although only a part of the brush can be placed near the cathode due to the large brush size. A brush anode also has very high surface area relative to that of the cathode, making it likely that the size of the brush is larger than it needs to be to produce maximum power densities. It has been shown in several studies with flat electrodes that changing the size of the anode relative to that of the cathode will affect power [3,7,8], but this type of study has not been conducted with brush anodes. Changing the size of the brush anode could reduce performance due to either less bacteria or to oxygen contamination of the anode.

Higher power densities in MFCs can be obtained by reducing internal resistance, making it important to understand the specific origins of the internal resistance. Components include solution resistance (electrode spacing, electrode area, and solution conductivity), charge transfer resistance of the electrodes (contact resistance and conductivity), and diffusion resistance (slow diffusion of chemical species). The total internal resistance can be obtained either from the linear portion of the polarization curve [1], or through analysis of electrochemical impedance spectra (EIS) [9]. In a previous study using EIS it was found that charge transfer resistance was the major component of the internal resistance in a brush anode MFC with a stainless steel mesh Pt-catalyzed cathode [10]. In two of the tests with different sized mesh, however, diffusion resistance predominated. In another study with a different type of MFC with an air cathode and a very large (brush) anode surface area relative to that of the cathode, diffusion resistance predominated in tests with several types of buffers at different concentrations [11]. The analysis of the EIS spectra was performed differently in these two studies: Zhang et al. [10] fit EIS data using equivalent circuits; Nam et al. [11] calculated the solution and charge trans-

* Corresponding author. Tel.: +1 814 863 7908; fax: +1 814 863 7908.
E-mail address: blogan@psu.edu (B.E. Logan).

0378-7753/$ – see front matter © 2011 Elsevier B.V. All rights reserved.
doi:10.1016/j.jpowsour.2011.07.040

fer resistances by fitting semi-circles to data in Nyquist plots, and diffusion resistance was deduced from the difference between the total internal resistance using the polarization slope analysis and the other two resistances. Thus, diffusion resistance was not independently evaluated in the latter case. In both of these previous studies only whole cell spectra were analyzed, and the individual charge transfer resistances of the electrodes were not investigated.

In this study the size of brush anodes was systematically varied in order to determine the minimum brush size that would affect power generation either through insufficient brush material or oxygen contamination. The brushes were trimmed from the side most distant from the cathode in order to test if removing the distant part of the brush would affect power generation. In order to better separate the effects of oxygen crossover and brush mass, MFCs were tested with the ends of the brushes set at three different distances from the cathode (0.4, 0.8 and 1.4 cm). In a high conductivity solution, increasing the distance between the anode and cathode should produce minimal changes in solution resistance. However, in low conductivity solutions, typical of domestic wastewaters, small changes in electrode spacing can produce large changes in internal resistance [12]. Therefore, the solution resistance was varied here by using three different concentrations of buffer to span a range of conductivities typical of wastewater and more optimized laboratory conditions. The effects of all of these changes were evaluated in terms of maximum power densities obtained from polarization data. The sources of internal resistance were evaluated using both the linear slope polarization and EIS methods. A new approach was used here to obtain the diffusion resistances from EIS spectra in order to independently calculate this component of the internal resistance.

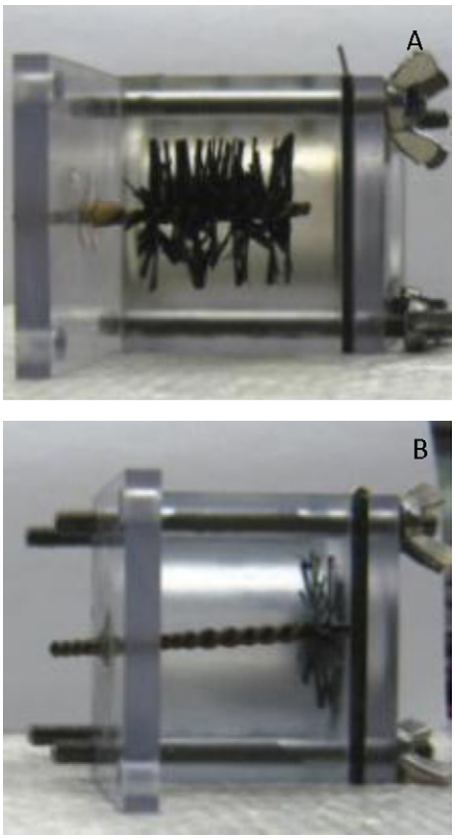

Fig. 1. MFC with full brush anode (A) and with 75% of the brush anode removed from the side farthest from the cathode (B).

2. Materials and methods

2.1. MFC reactor construction and operation

MFC's were single chamber 4 cm cube reactors made from Lexan, with a 28 mL cylindrical chamber [13]. Brush anodes (manufactured by Mill-Rose, Mentor, OH) were made from graphite fibers (25 mm diameter × 25 mm length; 0.4 g; 1150 cm^2 surface area; fiber type: PANEX 35 50K, Zoltek) twisted between two titanium wires (single wire: length, 5 cm; 17 gauge; #2 grade; Titanium Industries). The anodes were heat treated (450 °C for 30 min) [14] and placed with the wire in the center of the cylindrical chamber with the wire perpendicular to the cathode (Fig. 1). Cathodes were constructed from wet-proofed (30%) carbon cloth (type B, E-TEK) coated with carbon black, platinum (0.5 mg-Pt cm^{-2}), and Nafion binder on the side facing the electrolyte, and with a carbon black base layer and four polytetrafluoroethylene (PTFE) diffusion layers on the air side [15].

MFCs were inoculated with a 1:1 ratio of effluent from MFCs that had been operated for over 1 year and 50 mM phosphate buffer solution (PBS) with an organic substrate (1.0 g L^{-1} sodium acetate). The PBS contained: Na_2HPO_4, 4.58 g L^{-1}; $NaH_2PO_4{\cdot}H_2O$, 2.45 g L^{-1}; NH_4Cl, 0.31 g L^{-1}; KCl, 0.13 g L^{-1}; trace minerals, 12.5 mL L^{-1}; vitamins 5 mL L^{-1}) [16]. MFCs were re-inoculated after the voltage peaked and declined to less than 10% of the previous peak. After three cycles MFCs were then operated using only the substrate and buffer solution. MFCs with 8 mM or 25 mM PBS were inoculated with the same 1:1 ratio of MFC effluent and substrate buffer solution. The effluent from MFCs using 50 mM PBS solution and substrate buffer solution were diluted to 8 mM and 25 mM concentration and the inoculation procedures were the same as previously described. Once these reactors reached sustained peak voltages the effluent was collected and used to inoculate MFCs to be used in MFC experiments with 8 mM and 25 mM PBS using the same procedure as previously described. Characteristics of the three different media used in experiments were: 50 mM substrate buffer solution (pH = 7.1, conductivity = 7.8 mS cm^{-1}), 25 mM (pH = 7.1, conductivity = 3.5 mS cm^{-1}), and 8 mM (pH = 7.2, conductivity = 1.8 mS cm^{-1}). The solution was replaced when the voltage decreased to <10% of the peak voltage.

2.2. Experimental procedure

Two types of experiments were performed: progressive anode removal; and startup with reduced anode sizes.

Progressive anode removal: For the progressive anode removal experiments, nine MFCs were inoculated with full brush anodes and allowed to reach steady state conditions as evidenced by repeatable maximum voltages over three or more cycles. The MFCs were then tested with different electrode spacings (triplicate reactors). The anodes were sealed with epoxy at distances of 0.4 cm, 0.8 cm and 1.4 cm between the front tip of the brush anode facing the cathode, and the inner face of the cathode. Once an operational steady state was reached at the different electrode distances, brush fibers were removed incrementally from the anode starting at the side of the brush farthest from the cathode and moving towards the cathode (Fig. 1). For each increment of brush removal one and a half to three full spirals were removed using scissors as close as possible to the wire, in four to seven steps that reduced the brush mass by 10–30% each time. The fibers were dried in a furnace at 200 °C for 2 h, and weighed to determine the percent of the overall brush that had been removed. This procedure could have resulted in a small overestimation of the mass of brush removed due to biomass on the removed carbon fibers, although a biofilm was not visually apparent on the brushes. After anode material had been removed

the MFCs were allowed at least three feed cycles to return to a repeatable peak voltage.

Reduced anode startup: To assess the impact of anode material on startup time the maximum voltages produced were obtained for MFCs with three different buffer solutions (8 mM, 25 mM, and 50 mM PBS) with 0%, 50%, and 75% of the anode material removed at the start of the experiment. These MFCs were inoculated and operated as described above for the full brush anodes. The startup time was determined as that needed to produce a repeatable peak voltage over three cycles or more.

2.3. Analysis

The MFCs were operated with an external circuit containing a 1000 Ω resistor at room temperature (22 ± 3 °C). Voltage across the resistor was recorded every 20 min with a multimeter (Keithley Instruments, Cleveland, OH) and recorded on a computer. Electrochemical tests were performed using a potentiostat (BioLogic, VMP3) and analyzed with EC-Lab V10.02 software. Electrochemical tests included: linear sweep voltammetry (LSV), to determine power density and internal resistance; and electrochemical impedance spectroscopy (EIS), to determine components of internal resistance. EIS and linear polarization experiments were performed sequentially within an hour of each other to ensure the same working conditions for each experiment. The EC-Lab software was used to generate Nyquist and Bode plots from EIS data. These plots and circle fitting software were used to analyze and attribute specific portions of internal resistance to specific components of the MFCs.

LSV tests were conducted by setting the reactor at its open circuit potential (OCP) for 30 min, and scanning the voltage from −515 mV to −180 mV at a rate of 0.1 mV s^{-1} [17], with the anode as working electrode and cathode as the counter and reference electrode. Power density was calculated using $P = EI/A$, where A is the projected surface area of the cathode (7 cm^2). All experiments showed that the peak power density for the MFCs always occurred between the chosen start and end voltages, and therefore a broader range of voltages were not used in order to minimize analysis time. Total internal resistance was determined from the linear portion of the polarization data using the polarization slope method [1].

Electrochemical impedance spectroscopy (EIS) was performed separately on the anode and cathode, and on the whole cell. The AC amplitude was 10 mV and the frequency was varied from 100 kHz to 5 mHz with 5 steps per decade, and the external resistance was 1000 Ω. Two electrode experiments were performed on the whole cell with the anode as the working electrode and the cathode used as the counter and reference electrode. Three electrode experiments were performed with one electrode (anode or cathode) as the working electrode and the other electrode being the counter electrode, with a Ag/AgCl (+0.211 V vs. SHE) reference electrode. Potentials are reported vs. Ag/AgCl except as noted. Component resistances were summed to obtain the total EIS internal resistance. The whole cell experiments were supported by the specific electrode EIS measurements to correctly identify the anode and cathode contributions to total internal resistance. By including the external circuit during the EIS experiments the results reflect internal resistances present in the MFC under working conditions.

To determine the resistances associated with solution, charge transfer, and diffusion EIS data was analyzed using EC-Lab V10.02 software. Many studies have used equivalent circuit models (ECM) to determine the contributions from different resistances to the overall MFC resistance [9,10,18,19], however, there is rarely a direct physical relationship between the values of components in an ECM and the real system as coupled physical processes are complicated [20]. Instead of using ECM to find internal resistance from EIS data, circle fit software, Nyquist plots, and Bode plots were interpreted

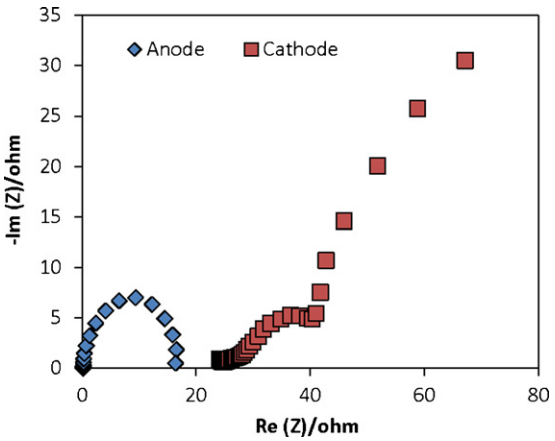

Fig. 2. Nyquist plot of EIS data for anode (diamonds) and cathode (squares). Anode impedance data shows charge transfer resistance as semicircle. Cathode impedance data shows charge transfer resistance as a small semicircle and diffusion resistance at low frequency as a finite diffusion layer. Each data point is the response of the system at a specific frequency. The first data point on the left is the response at 100 kHz followed by responses to scanned frequencies to 5 mHz which is the last data point on the right.

to arrive at resistance values as described below. Nyquist plots, or complex plane plots, present the data for the range of frequencies explored as the imaginary part of the impedance, −Im (Z), plotted against the real part of the impedance, Re(Z). Bode plots of log|Z| and phase angle vs. the log of frequency represent the frequency variation of the real and imaginary impedance of the system [21].

The method used to determine individual component resistances can be demonstrated by the following examples. Anode impedance was obtained using circle fit software, where the diameter of the first (high frequency) circle is charge transfer resistance (AR_{CT}). In the example shown in Fig. 2, AR_{CT} = 18 Ω. Preliminary analyses showed that cathode and whole cell EIS data had similar responses to frequency data comprised of charge transfer resistance and diffusion resistance, and that both responses were more difficult to fit using an ECM. Cathode EIS data typically showed a small cathode charge transfer resistance (CR_{CT}) at high frequencies and a finite diffusion resistance at low frequencies (Fig. 2). Circle fitting software was therefore used to determine the CR_{CT}, and in the example (Fig. 2) CR_{CT} = 23 Ω. Using EIS on the whole cell, the solution resistance was found at high frequencies where the impedance data crosses the Re(Z) axis (Fig. 3A, point 1), and in the example shown R_S = 48 Ω. Total charge transfer resistance was determined from the semicircle in this example to be 43 Ω at middle frequencies (Fig. 3A, point 2), and total diffusion resistance was calculated from low frequency data to be 110 Ω (Fig. 3A, point 3). To validate R_{CT} from each whole cell, the R_{CT} was compared to the summed anode and cathode resistances, with values typically within one to two ohms. Diffusion resistance (R_D) was defined as the last value obtained in the lowest frequency data based on the assumption that the impedance was steady at this point (Fig. 2B, point 3). To validate this assumption, the Bode plot was examined to ensure that there was a plateau in the low frequency range (left side) of the plot (Fig. 3B). Total whole cell impedance values were determined from the projected point of intersection of the Nyquist plot and the Re(Z) axis.

3. Results

3.1. Startup time

Reducing the size of the anode increased the startup time for MFCs at all three buffer concentrations (50 mM, 25 mM and 8 mM

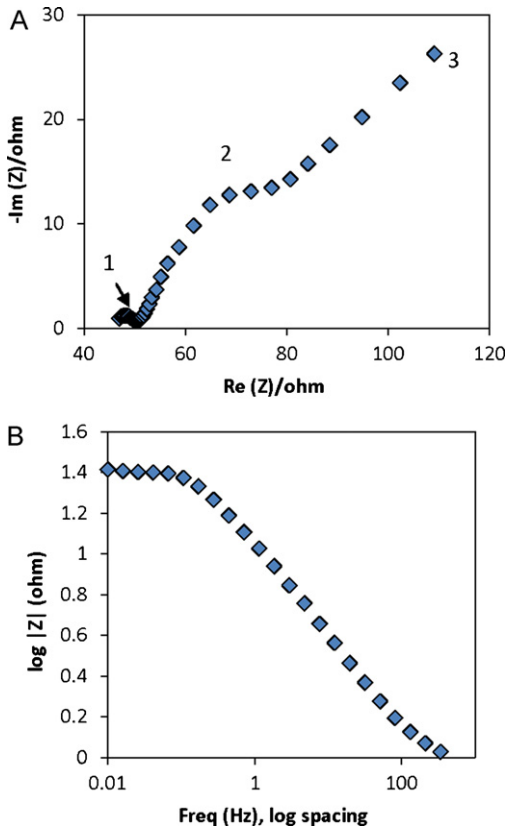

Fig. 3. Typical whole cell impedance data presented in Nyquist plot (A). (1) Solution resistance of 48 Ω found from first intersection of Nyquist plot and *x*-axis, (2) charge transfer resistance of 43 Ω determined from circle fit of curved part of Nyquist plot, (3) diffusion resistance of 110 Ω. (B) Typical Bode Plot showing impedance values for each frequency used during EIS experiments.

PBS) (Fig. 4). Startup time with a full brush and 50% of brush removed was 9 days for MFCs using 50 mM PBS, and 8 ± 1 days at 25 mM. The startup time increased to 13 days when a brush was used that initially had 80% of brush removed in 50 mM PBS, and 14 days with 25 mM PBS. Lowering the concentration of the substrate buffer solution to 8 mM in order to produce solution conductivity similar to real wastewater did not affect startup of anodes with the full brush (9 days), but it increased startup time to 21 days when 50% or 80% of the brush material had been removed prior to inoculation.

3.2. Power density

Maximum power densities increased with the concentration of buffer solution as expected [22], with values of 460 ± 70 mW m^{-2} (8 mM), 782 ± 115 mW m^{-2} (25 mM), and 940 ± 100 mW m^{-2} (50 mM). Power density increased as electrode spacing decreased, but only by 15 ± 5% when the electrode spacing moved from 1.4 cm to 0.4 cm. Removal of anode brush material over time decreased power only after ~75% of the material was removed (Fig. 5). There was no systematic trend among the different configurations as a function of electrode spacing and PBS concentration when power decreased for 75% brush removal. There was a slightly greater impact of brush removal for MFCs with close electrode spacing at 25 mM and 50 mM PBS, but not with the 8 mM PBS. The largest observed decrease in power was 35%, or from 930 ± 50 mW m^{-2} (full brush) to 615 ± 50 mW m^{-2} (75% brush removed), for the intermediate PBS concentration (25 mM) and 0.4 cm electrode spacing.

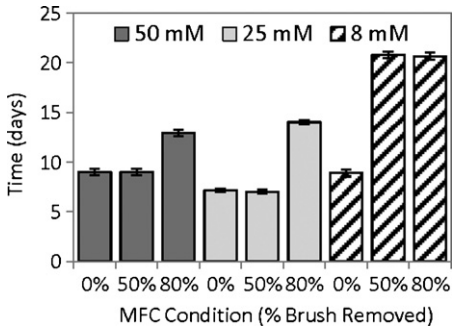

Fig. 4. Startup time for varying percentage of brush anode removed for 50, 25, and 8 mM PBS substrate MFCs.

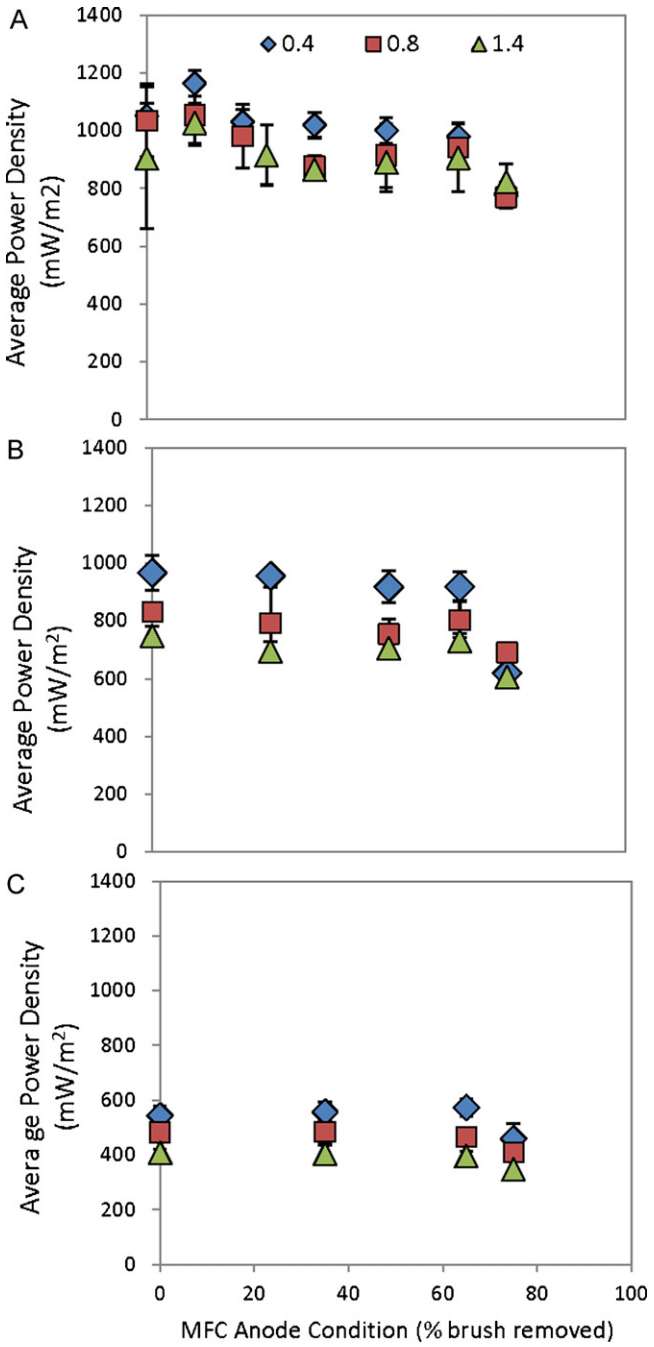

Fig. 5. Peak power densities for MFCs with different spacing between electrodes and percentage of anode material progressively removed. (A) 50 mM PBS, (B) 25 mM PBS, (C) 8 mM PBS.

The MFCs with 0.8 cm and 1.4 cm electrode spacing decreased in power by only 18 ± 1% for 75% of brush removed at 25 mM PBS concentration. The power densities decreased by 27% with 50 mM PBS for 0.4 cm and 0.8 cm electrode spacing, but only by 10% decrease with a 1.4 cm spacing. Power decreased by only 15% with 8 mM PBS for all electrode distances. This suggests that small differences in the biofilm distribution on the remaining anode brush material were probably an important factor in the resulting power production with a large amount of the brush removed.

3.3. Internal resistance

Diffusion resistance was the dominant component of internal resistance for all electrode spacings and PBS concentrations examined. Typical results are shown in Fig. 6 for a 0.4 cm electrode spacing at the three different buffer concentrations. The internal resistance increased with electrode spacing (from 0.4 cm to 1.4 cm) and as solution conductivity decreased (from 7.8 mS cm^{-1} to 1.8 mS cm^{-1}). The increase in resistance was due to increased solution and diffusion resistances. Changes due to solution resistance can be determined by comparing MFCs that only differ by electrode spacing. Solution resistance was responsible for a 20 ± 5% (25 mM and 50 mM PBS) to 35 ± 5% (8 mM PBS) of the total internal resistance. Diffusion resistance was the dominant component of internal resistance for MFCs under all experimental conditions accounting for 50–62% of the total. Charge transfer resistance at both electrodes remained the same (within a standard deviation) for all experimental conditions with one exception; a large increase in AR_{CT} was observed in the MFC experiments performed with a 50 mM buffer and 0.8 cm electrode spacing. The other increases in total internal resistance were due to slight increase in solution resistance and diffusion resistance. It should be noted that all resistance values reported here are specific to the operating conditions investigated during this study.

The total internal resistances obtained from the slopes of the polarization data compare well on a case by case basis in all experiments with the sum of the resistances calculated using EIS. Examples of the individual values are shown in Fig. 6 for the MFCs with 0.4 cm electrode spacing. To further examine if there was any bias in the internal resistance produced by EIS compared to the slope of the polarization data, all data were compared on the basis of maximum power (Fig. 7). This result shows that the two methods compare very well, with the EIS method on average producing values similar within the range of error of 5 ± 6% (50 mM), 5 ± 3% (25 mM), and 4 ± 2% (8 mM) larger than those obtained with the linear polarization slope method (Fig. 6). From these results it can be concluded that the internal resistance determined from EIS was not missing any significant component of the total resistance and can be used to determine which component of internal resistance is dominant.

Additional tests were conducted using EIS spectra under open circuit conditions in order to compare results here with those obtained in previous studies conducted with OCP conditions. The summed resistances were much larger under OCP than working cell conditions, with 550 Ω for OCP conditions and 140 Ω compared to working conditions (Fig. 8). With an open circuit, the different components of the internal resistance are measured under conditions where there is very little charge dispersal, and therefore nearly infinite impedance. As a result, the rate of chemical reactions are very

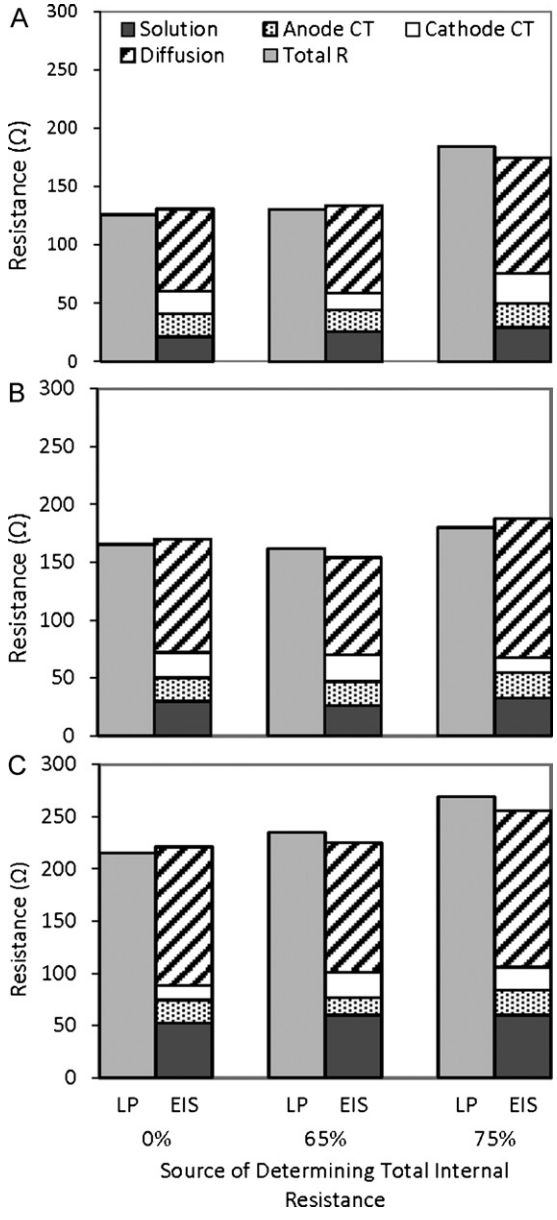

Fig. 6. Comparison of average total internal resistance using slope of linear polarization curve (LP) method and individual component EIS method of 50 mM PBS MFCs from progressive anode removal experiments with 0.4 cm electrode spacing. (A) 50 mM PBS, (B) 25 mM PBS, and (C) 8 mM PBS.

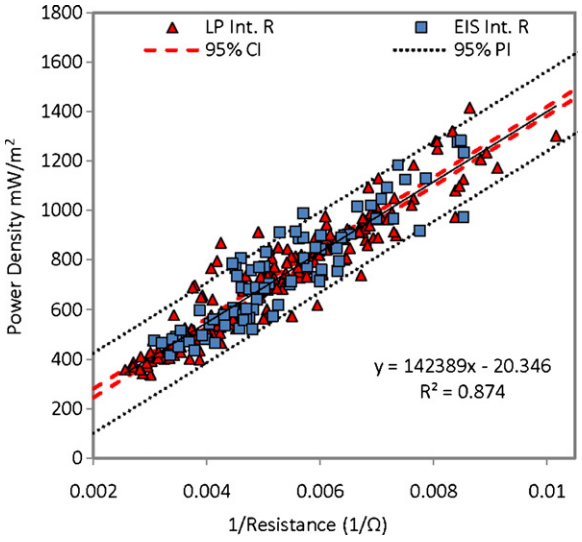

Fig. 7. Distribution of power density and related internal resistance with estimated trend line as distribution mean and 95% confidence interval (CI) and 95% prediction interval (PI) for 50 mM, 25 mM and 8 mM MFCs.

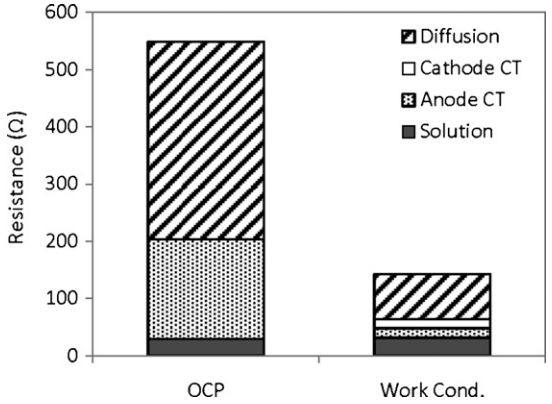

Fig. 8. Internal resistance of a single MFC determined from EIS experiments performed at open circuit potential and working condition potential. Internal resistances are divided into contributions of individual component resistances.

low due to a lack of appreciable current, leading to very low rates of charge dispersal which are dominated by diffusion. Thus, the EIS analysis under OCP conditions results in conditions that have little relationship to those occurring under working conditions. This indicates that EIS should only be applied under working cell conditions in order to determine the components of the internal resistance that are relevant to MFC operation.

4. Discussion

Through the progressive anode material removal experiments it was shown that much of the anode material (~65%) could be removed from fully acclimated anodes without adversely affecting power generation (Fig. 5). However, reactors took longer to startup (to produce consistent maximum voltages) when operated with brushes that always had 75% less fibers. It is likely that during startup oxygen diffusion through the cathode affected the development of an exoelectrogenic biofilm, with the impact of oxygen being more severe for the trimmed brushes than the full brushes. Following inoculation, we can assume the concentration of bacteria on the anode is initially low. As a result, on the anode surface nearest to the cathode there will be insufficient consumption of oxygen to keep that portion of the anode under sufficiently anoxic conditions needed for exoelectrogenic activity. When using a full brush anode, we speculate that bacteria distant from the cathode would exist under more anoxic conditions than those near the cathode, allowing exoelectrogenic consortia to develop on the more distant part of the anode and to generate current. As the mass of biofilm on the anode increases over time for both trimmed and full brushes, then more of the brush could achieve sufficiently anoxic conditions through scavenging oxygen diffusing into the brush, allowing improved current generation. This scenario would explain the slower startup of the trimmed brushes based on the absence of bacteria sufficiently distant from the cathode to produce current. Startup would be delayed for the trimmed brush until sufficient biofilm could consume the oxygen, thereby allowing the growth of exoelectrogenic bacteria and current generation.

The longest startup time that was needed (21 days compared to ~8 days for other conditions) was the MFCs operated with 8 mM PBS with 50 or 75% of the brush initially removed (Fig. 4). The low solution conductivity (1.8 mS cm^{-1}) results in a high internal resistance, and therefore this limits current production compared to tests with higher solution conductivities. The lower current production means that an exoelectrogenic biofilm will develop more slowly. Thus, the combined high internal resistance and lack of brush material distant from the cathode created the poorest conditions for startup of the reactor. Wastewaters typically have low conductivities, making this low conductivity situation during startup the most relevant condition for practical applications. Slow startup with the smaller brushes suggests that brushes larger than those needed to sustain high power densities may be needed to ensure faster startup, and perhaps more stable operation, of the MFC with low conductivity wastewaters unless other methods can be found to improve startup. Recent tests with several organic and inorganic amendments have failed to identify methods to reduce startup time in MFCs treating domestic wastewater [23].

EIS analysis of the reactor showed that diffusion resistance was the single greatest contributor to the total internal resistance. Whole cell EIS results showed a significant increase in R_D as solution conductivity decreased and electrode spacing increased, in agreement with cathode EIS results. This finding of a high diffusion resistance is in agreement with results by Nam et al. [11] based on a similar method of fitting Nyquist data using circles to identify the charge transfer and solution resistances. However, conclusion is different than that of Zhang et al. [10], where it was found that charge transfer resistance dominated when EIS data was analyzed using an equivalent circuit method. The study conditions were not completely comparable to those used here, however, as different types of cathodes were used in that study. In addition, in Zhang et al.'s [10] study there were additional cases where the diffusion resistance was unexpectedly much larger than other resistances. The consistency of the approach used here, and the good comparison with internal resistances based on the slope of polarization data, suggests that the Nyquist plot approach may be more suitable for analysis of MFCs than the equivalent circuit method. It was also found here that diffusion resistance varied inversely with solution conductivity, in agreement with findings by Aaron et al. [24]. They reported an increase in cathode and total internal resistance with a decrease in anolyte ionic strength. Our results also suggest that the assumption made by Nam et al. [11] that diffusion resistance can be calculated as the difference between total IR and the sum of the charge transfer and solution resistance.

Charge transfer resistance at both electrodes remained the same within a standard deviation for all experimental conditions. EIS results showed that once an anodic consortium was established and the working condition charge transfer resistance reached a steady value, changing solution conductivity and electrode spacing had little impact on this component of internal resistance. This finding was in agreement with a study by Borole et al. [25] where they reported that anode impedance decreased during biofilm growth (from $296 \pm 137\ \Omega$ to $1.41 \pm 0.13\ \Omega$) and then became constant with an acclimated biofilm. This shows that anode charge transfer resistance is a useful method for evaluating the stability of the anode biofilm for power production.

5. Conclusions

In general, currently used carbon fiber brush anodes are usefully overdesigned when considering surface area. It was shown here that up to 65% of the brush material could be removed without decreasing power generation. However, decreasing anode surface area has a negative impact on startup time especially for MFCs with solution characteristics mimicking wastewater. The dominant component of internal resistance, R_D, is not decreased by providing a large surface area at the anode. Providing a large amount of anode surface area does not alleviate the need to optimize buffer concentration and distance between electrodes. It has been shown that EIS can be used to determine individual component resistances without missing any significant sources of internal resistance.

Acknowledgement

This research was supported by funding through the King Abdullah University of Science and Technology (KAUST) (Award KUS-I1-003-13).

References

[1] B.E. Logan, Microbial Fuel Cells, Wiley-Interscience, Hoboken, N.J., 2008.
[2] A. Rinaldi, B. Mecheri, V. Garavaglia, S. Licoccia, P. Di Nardo, E. Traversa, Energ. Environ. Sci. 1 (2008) 417–429.
[3] B. Logan, S. Cheng, V. Watson, G. Estadt, Environ. Sci. Technol. 41 (2007) 3341–3346.
[4] M. Zhou, M. Chi, J. Luo, H. He, T. Jin, J. Power Sources 196 (2011) 4427–4435.
[5] S. Cheng, H. Liu, B.E. Logan, Electrochem. Commun. 8 (2006) 489–494.
[6] S. Hays, F. Zhang, B.E. Logan, J. Power Sources, (2011), doi:10.1016/j.jpowsour.2011.06.027.
[7] Y. Zuo, S. Cheng, D. Call, B.E. Logan, Environ. Sci. Technol. 41 (2007) 3347–3353.
[8] S.-E. Oh, B. Logan, Appl. Microbiol. Biotechnol. 70 (2006) 162–169.
[9] Z. He, F. Mansfeld, Energ. Environ. Sci. 2 (2009) 215–219.
[10] F. Zhang, M.D. Merrill, J.C. Tokash, T. Saito, S. Cheng, M.A. Hickner, B.E. Logan, J. Power Sources 196 (2011) 1097–1102.
[11] J.Y. Nam, H.W. Kim, K.H. Lim, H.S. Shin, B.E. Logan, Biosens. Bioelectron. 25 (2010) 1155–1159.
[12] R.A. Rozendal, H.V.M. Hamelers, K. Rabaey, J. Keller, C.J.N. Buisman, Trends Biotechnol. 26 (2008) 450–459.
[13] H. Liu, B.E. Logan, Environ. Sci. Technol. 38 (2004) 4040–4046.
[14] Y. Feng, Q. Yang, X. Wang, B. Logan, J. Power Sources 195 (2010) 1841–1844.
[15] S. Cheng, H. Liu, B. Logan, Electrochem. Commun. 8 (2006) 489–494.
[16] S.A. Cheng, B.E. Logan, Electrochem. Commun. 9 (2007) 492–496.
[17] S.B. Velasquez-Orta, T.P. Curtis, B.E. Logan, Biotechnol. Bioeng. 103 (2009) 1068–1076.
[18] R.P. Ramasamy, V. Gadhamshetty, L.J. Nadeau, G.R. Johnson, Biotechnol. Bioeng. 104 (2009) 882–891.
[19] R.P. Ramasamy, Z.Y. Ren, M.M. Mench, J.M. Regan, Biotechnol. Bioeng. 101 (2008) 101–108.
[20] D.A. Harrington, P. van den Driessche, Electrochim. Acta, (2011), doi:10.1016/j.electacta.2011.01.067.
[21] C.H. Hamann, A. Hamnett, W. Vielstich, Electrochemistry, 2nd ed., Wiley-VCH, Weinheim, Germany, 2007.
[22] F. Li, Y. Sharma, Y. Lei, B. Li, Q. Zhou, Appl. Biochem. Biotechnol. 160 (2010) 168–181.
[23] G. Liu, M.D. Yates, S. Cheng, D.F. Call, D. Sun, B. Logan, Bioresour. Technol. 102 (2011) 7301–7306.
[24] D. Aaron, C. Tsouris, C.Y. Hamilton, A.P. Borole, Energies 3 (2010) 592–606.
[25] A.P. Borole, D. Aaron, C.Y. Hamilton, C. Tsouris, Environ. Sci. Technol. 44 (2010) 2740–2744.